Available online at www.sciencedirect.com
SCIENCE DIRECT
Computers and Electronics in Agriculture 46 (2005) 45–70
Computers and electronics in agriculture
www.elsevier.com/locate/compag

Soil properties influencing apparent electrical conductivity: a review

Shmulik P. Friedman*

The Institute of Soil, Water and Environmental Sciences, Agricultural Research Organization, The Volcani Center, Bet Dagan 50250, Israel

Abstract

The most common method for in situ assessment of soil salinity, namely the electrical conductivity (EC) of the soil solution (EC_w), is to measure the apparent electrical conductivity (EC_a) and volumetric water content (θ) of the soil and apply measured or predicted $EC_a(EC_w, \theta)$ calibration curves. The water content and electrical conductivity of a soil solution are indeed the major factors affecting its apparent electrical conductivity, which justifies the assessment of salinity from apparent EC measurements. However, the $EC_a(EC_w, \theta)$ relationship depends on some additional soil and environmental attributes affecting the soil EC_a. Non-spherical particle shapes and a broad particle-size distribution tend to decrease EC_a, and when non-spherical particles have some preferential alignment in space, the soil becomes anisotropic, i.e., its EC_a depends on the direction in which it is measured. The electrical conductance of adsorbed counterions constitutes a major contribution to the EC_a of medium- and fine-textured soils, especially under conditions of low solution conductivity. In such soils and with such salinity levels, the temperature response of the soil EC_a should be stronger than that of its free solution, and care should be taken when extrapolating from field-measured EC_a values to obtain the EC_a at a given temperature. The above-mentioned and other secondary findings should, on one hand, indicate some limitations for the application of existing EC_a–EC_w models, and, on the other hand, can serve as guidelines for further development of such essential models.

Keywords: Apparent (effective) electrical conductivity; Soil salinity

* Tel.: +972 3 968 3424; fax: +972 3 960 4017.
E-mail address: vwsfried@agri.gov.il.

0168-1699/$ – see front matter © 2004 Elsevier B.V. All rights reserved.
doi:10.1016/j.compag.2004.11.001

1. Introduction

Electrical conductivity (EC) of soil solution (σ_w) is a reliable indicator of its solute (cation or anion) concentration with 1 dS/m approximately equivalent to 10 meq/L (U.S. Salinity Laboratory Staff, 1954). Measurements of effective (bulk) electrical properties of soils started at the end of 19th century (e.g., Briggs, 1899; Wenner, 1915; Smith-Rose, 1933; Archie, 1942), and the practice of measuring effective (apparent) electrical conductivity of the soil, EC_a (or σ_a), as a step in assessing soil salinity, has been spreading continuously since the 1970s (Rhoades and Ingvalson, 1971; Rhoades and van Schilfgaarde, 1976) as reviewed by Rhoades et al. (1999) and Hendrickx et al. (2002). In the last two decades, another significant incentive for the determination of soil solution EC from EC_a measurements has arisen from the possibility of simultaneous measurements of EC_a and soil volumetric water content (θ) by the time domain reflectometry (TDR) method (Topp et al., 1980; Dalton et al., 1984; Robinson et al., 2003). The water content (θ) and σ_w are indeed the major factors affecting σ_a, which provides the justification for using the $\sigma_w(\sigma_a, \theta)$ assessment. However, the $\sigma_w(\sigma_a, \theta)$ relationship depends on additional soil and environmental attributes, which limits the predictability of general, theoretical $\sigma_w(\sigma_a, \theta)$ relationships and often necessitates performing laborious, site-specific $\sigma_w(\sigma_a, \theta)$ (or $\sigma_a(\sigma_w, \theta)$) calibrations. A general $\sigma_a(\sigma_w, \theta)$ model that relies on easily attainable soil parameters has not yet been proposed, and it is not the purpose of this review to do so.

This review discusses how and to what extent various soil and environmental attributes affect the $\sigma_a(\sigma_w, \theta)$ relationship. This is meant to help practitioners choose among, and cautiously apply, one of the existing empirical and theoretical $\sigma_a(\sigma_w, \theta)$ models, and assist researchers to further develop such models. In Section 2, I define the physical $\sigma_a(\sigma_w, \theta)$ problem, set some limitations, and briefly mention several different concepts for its analysis. In Section 3, I review and discuss the experimental and theoretical findings regarding the effects of soil and environmental attributes on the EC_a of water-saturated and unsaturated soils.

2. The effective electrical conductivity problem

The effective electrical conductivity referred to in this article, EC_a (σ_a), is the "quasi-static" conductivity in the frequency range from dc to approximately 1 kHz. The commonly used frequency range for EC_a determination in the field is about 100 Hz to several kHz, because at lower frequencies, electrode polarization interferes with the readings and at higher frequencies (kilo- to megahertz), σ_a is no longer constant at the dc value, but increases with frequency (a phenomenon termed dispersion). Furthermore, high-frequency conductivity meters are expensive.

An unsaturated soil is considered to be a three-phase, solid–water–air system. The minerals constituting the solid phase of soils and rocks are non-conducting ($\sigma_s = 0$), as, of course, is the air ($\sigma_A = 0$), so that the only conducting phase is the aqueous solution, which has an intrinsic specific electrical conductivity of σ_w (S/m). For these reasons, in certain circumstances, especially when σ_w can be reliably evaluated, EC_a measurements can also be used for evaluating volumetric water contents (θ) and, as a special, two-phase case, the porosity

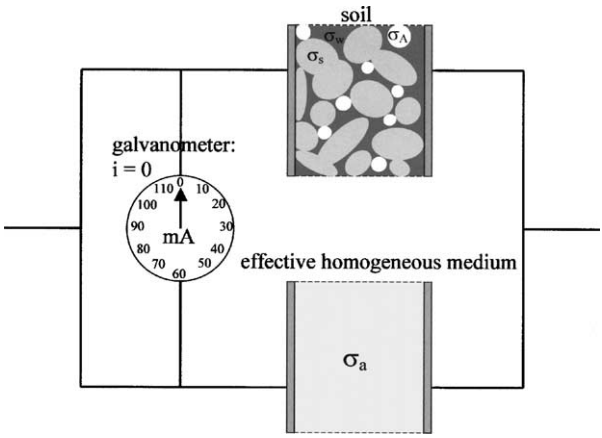

Fig. 1. An unsaturated soil with a conducting aqueous phase of specific electrical conductivity of σ_w and non-conducting solid ($\sigma_s = 0$) and gaseous ($\sigma_A = 0$) phases, and a homogeneous, single-phase material of the same effective (apparent) electrical conductivity, σ_a.

(n) of water-saturated soils and rocks. An unsaturated soil is an example of a mixture of several constituents that have differing intrinsic conductivities (σ_i), and only one of which conducts ($\sigma_w > 0$) in our case. In addition to differing in their single-phase conductivities, the components (phases) also differ in their volumetric fractions, shapes, and orientations. The effective (apparent) electrical conductivity of the three-phase mixture (σ_a, S/m) can be defined in more than one way; Torquato (2002, p. 359), for example, defines it as the relation between the volume-averaged electrical field ($\langle \boldsymbol{E} \rangle$, V/m) and the volume-averaged electrical current density ($\langle \boldsymbol{J} \rangle$, A/m^2):

$$\langle \boldsymbol{J} \rangle = \sigma_a \langle \boldsymbol{E} \rangle \tag{1}$$

Here we will adopt a more general and practical approach to defining σ_a (EC$_a$): the effective EC of a soil is defined as the conductivity of a homogeneous, single-phase material that elicits the same response in a measuring device (see Fig. 1). The reader is reminded that we refer to a representative volume of soil that is statistically homogeneous within the spatial resolution of the measuring device; we do not deal with spatial variability of the soil properties, which is discussed elsewhere in this issue (Lesch, 2005; Wraith et al., 2005). When the EC$_a$ of a homogeneous wet soil is being measured with a 10-cm long four-probe array, for example, the sub-millimeter-scale heterogeneities of the soil particles, water bodies, and air volumes are invisible to the EC meter and the device observes the sample as a homogenous entity with a single effective conductivity. If there were centimeter-scale layerings such as in the hydrostatic distribution of water content along the vertical four-probe array, or other heterogeneities with centimeter-long correlation lengths in the soil sample, those heterogeneities would affect the measured conductivity that would no longer match the above-defined effective conductivity.

There are several theoretical approaches for evaluating the effective EC (σ_a) of mixtures for which the volumetric fractions and single-phase permittivities of the constituents, and

other relevant geometrical and interfacial attributes, are known. Most of these methods for calculating σ_a fall into one of the two major conceptual categories: discrete resistor network models and continuum mean field theories.

The resistor network models deal only with the network of soil pores that can be occupied by either the liquid or the gaseous phase. With this approach, the conducting soil is replaced with an equivalent network of diverse resistors. Similar to the modeling of other transport properties, the resulting effective EC depends on the topology (connectivity) of the network and on the distribution of the resistances that decorate the bonds of the networks (Fatt, 1956; Friedman et al., 1995). The mathematical formulation of the problem results in Kirchoff's second electrical circuit law, to be solved either by a direct method involving matrix inversions (Friedman and Seaton, 1996) or by approximate methods that involve concepts such as effective medium approximations (Kirkpatrick, 1973), position-space renormalization (Kadanoff, 1966; Sahimi et al., 1983; Friedman et al., 1995), critical path analysis (Ambegaokar et al., 1971; Friedman and Seaton, 1998; Friedman and Jones, 2001), and related percolation concepts (Stauffer and Aharony, 1992; Sahimi, 1994).

As opposed to discrete lattice models, the mean field theories deal with the actual, continuous three-dimensional structure of the multiphase medium or with its idealized geometrical description. The evaluation of σ_a involves solving the electrostatic problem, namely the Laplace equation for the electrical potential, while conserving the continuity of the potential and the normal flux vectors on the interfaces between the various phases with their differing conductivities (Sihvola, 1999; Torquato, 2002). For real multiphase media such as wet soils, the Laplace equation can be solved by numerical methods, if their complex geometry can be reliably characterized and discretized (e.g., Adler et al., 1992). Another option is to refer to a simplified geometry of some common representative quantifiers and to solve the electrostatic problem for the transformed medium. An exact analytical solution to the Laplace equation does not exist even for the most simplified mixture geometry one could conceive. Therefore, the common practice is to apply some approximating assumptions regarding the spatial structure of the electrical fields in the various phases, a concept usually termed mean field theory. The three most common mean field theories differ in their weighting of the effects of the neighboring particles on the internal field of a reference particle. In the context of the electrical conductivity, they are usually termed: Maxwell (1881) model, the symmetric effective medium approximation (Bruggeman, 1935), and the coherent potential (CP) approximation (e.g., Tsang et al., 1985).

3. Factors affecting the apparent electrical conductivity of the soil

There are many factors that affect EC_a; the major ones discussed here can be grouped into three categories. Those in the first category describe the *bulk soil* and define the respective volumetric fractions occupied by the three phases and possible secondary structural configurations (aggregation): porosity (n), water content (θ), and structure. Factors in the second category are the important *solid particle* quantifiers, which are relatively time-invariable: particle shape and orientation, particle-size distribution, cation exchange capacity (CEC), and wettability. Factors in the third category are the relevant *soil solution* attributes, and as

these change quickly in response to alterations in management and environmental conditions, we may also call them *environmental* factors: ionic strength (σ_w), cation composition (sodium adsorption ratio, SAR $\equiv (Na^+)/((Ca^{2+} + Mg^{2+})/2)^{1/2}$), and temperature.

As stated above, the soil solution is the only conducting phase, which is why its volumetric fraction (θ) and conductivity (σ_w) are the two dominant factors in determining EC_a. Nevertheless, the geometry and topology of the aqueous phase are determined by the solid-phase attributes. Furthermore, the contribution of the adsorbed cations to the overall soil EC_a, significant for medium- and fine-textured soils, is also determined mostly by the soil's cation exchange capacity, which is a solid-phase attribute.

The above-mentioned 10 major factors do not, of course, act separately, and it is impossible to discuss them one by one without referring to the combined effects of several factors. Also, the major factor affecting the EC_a of unsaturated soils, i.e., their water content, obscures the secondary effects of their geometrical and also other interfacial attributes. Therefore, the major part of this review, the discussion of the relevant factors and their effects, is divided in Sections 3.1 and 3.2: the first deals with two-phase, water-saturated soils ($\sigma_a(\sigma_w, n)$), and the second with three-phase, unsaturated soils ($\sigma_a(\sigma_w, \theta, n)$). The three-phase problem, $\sigma_a(\sigma_w, \theta, n)$ is, of course, more relevant to agricultural soils but, unfortunately, it is also more complex than the two-phase $\sigma_a(\sigma_w, n)$ problem. As a result of the conceptual and experimental difficulties concerning the $\sigma_a(\sigma_w, \theta, n)$ relationship of unsaturated soils, the available reliable experimental evidence and our understanding of the effects of the geometrical and interfacial attributes of the solid phase are more extensive for the two-phase, water-saturated soil case than for the other. Therefore, in the present review, I have chosen to place somewhat more than usual emphasis on the discussion of factors that affect the EC_a of water-saturated soils. For further discussion of the EC_a of unsaturated soils, readers are referred to other recent publications (Rhoades et al., 1999; Hendrickx et al., 2002) including other articles in this special issue (Corwin and Lesch, 2005; Lesch, 2005).

3.1. Water-saturated soils

Most people measuring σ_a for evaluating the porosity (n) or solution conductivity of water-saturated soils and rocks still use Archie's empirical law (Archie, 1942):

$$\frac{\sigma_a}{\sigma_w} \equiv \frac{1}{F} = n^m, \tag{2}$$

which describes the reduced EC, σ_a/σ_w (the reciprocal of the commonly used formation factor, F), with m being a material-dependent empirical exponent. Archie (1942) found characteristic m values of 1.3 for unconsolidated sands and 1.8–2.0 for consolidated sandstones. Since m increases with cementation, Archie termed it the cementation index. In many later studies, partially reported in Table 1, Archie's law was found to hold for various porous media, with exponents ranging from 1.2 to about 4.0. In consolidated media, the effect of cementation on m was demonstrated by several researchers who compared non-fused ($m \approx 1.35$–1.4) and fused ($m \approx 1.5$–1.8) spherical particles of uniform size (Table 1). The porosity of consolidated, cemented media can be very low, and usually it is not constructive to describe their $\sigma_a/\sigma_w(n)$ relationships with a single m value. For consolidated media,

Table 1
Archie's law exponents (m) of different consolidated and non-consolidated media, as published in the literature, or calculated from reported $\sigma_a/\sigma_w(n)$ data

Medium	Porosity range	m (Archie's exponent)	Reference
Clean sand	0.12–0.35	1.3	Archie (1942)
Consolidated sandstones	0.12–0.40	1.8–2.0	
Glass spheres	0.37–0.40	1.38	Wyllie and Gregory (1955)
Binary sphere mixtures	0.147–0.29	1.31	
Cylinders	0.33–0.43	1.47	
Disks	0.34–0.45	1.46	
Cubes	0.19–0.43	1.47	
Prisms	0.36–0.52	1.63	
8 marine sands	0.35–0.50	1.39–1.58	Jackson et al. (1978)
Glass beads (spheres)	0.33–0.37	1.20	
Quartz sand	0.32–0.44	1.43	
Rounded quartz sand	0.36–0.44	1.40	
Shaley sand	0.41–0.48	1.52	
Shell fragments	0.62–0.72	1.85	
Fused glass beads	0.02–0.38	1.50	Sen et al. (1981)
Fused glass beads	0.10–0.40	1.7	Schwartz and Kimminau (1987)
Sandstone	0.05–0.22	1.9–3.7	Doyen (1988)
Polydisperse glass beads	0.13–0.40	1.28–1.40	de Kuijper et al. (1996)
Fused glass beads	0.10–0.30	1.6–1.8	Pengra and Wong (1999)
Sandstones	0.07–0.22	1.6–2.0	
Limestones	0.15–0.29	1.9–2.3	
Syporex®	0.80	3.8	Revil and Cathles (1999)
Bulgarian altered tuff	0.15–0.39[a]	2.4–3.3	Revil et al. (2002)
Mexican altered tuff	0.50[a]	4.4	
Glass beads	0.38–0.40	1.35	Friedman and Robinson (2002)
Quartz sand	0.40–0.44	1.45	
Tuff particles	0.60–0.64	1.66	

[a] Connected (inter-granular) porosity.

the best-fitting m usually increases with decreasing porosity. Doyen (1988), for example, obtained a best fit with $m = 1.9$ for samples of Fontainebleau sandstones with $n > 0.10$, and for $m = 3.7$ for those with $n < 0.10$. The highest m values listed in Table 1 were measured in a highly porous ($n = 0.8$), artificial porous medium (Syporex®, $m = 3.8$) comprised of large spherical pores interconnected by narrow throats, which is perhaps representative of some igneous rocks, and in a Bulgarian tuff ($m = 4.4$) containing secondary clay minerals and zeolites. Aggregated soils of a bimodal pore size distribution are also expected to be characterized by large values of the m exponent in conditions where both the intra- and inter-aggregate pores contribute significantly to the overall electrical conductivity.

For most granular media, particle shape is the major factor affecting $\sigma_a/\sigma_w(n)$: m increases from about 1.35 for spheres to about 1.65 for prismatic and angular tuff particles (Table 1). A detailed examination of a specific medium can reveal a few interesting features: for mono-sized spheres, m increased systematically from 1.368 to 1.375 as the porosity increased from 0.368 to 0.402 and this trend of m increasing with increasing n was found to be characteristic of other particle shapes also (Wyllie and Gregory, 1955). The tortuosity of porous and granular media decreases with increasing n; therefore, Archie's m should not be

regarded as a tortuosity quantifier. The effect of particle size distribution is consistent with the above; de Kuijper et al. (1996) found $m = 1.40$ for packed uniform spheres ($n = 0.40$), and m decreased to 1.28 for the polydisperse, $n = 0.13$, packing. Through the years, there have been several attempts to re-derive Archie's empirical law theoretically, e.g., by percolation theory (Balberg, 1986) and a statistical network model that accounted for compaction (Jonas et al., 2000), but these derivations are not general enough for real granular and consolidated media. Nevertheless, we recommend using Archie's Law, especially for soils and consolidated rocks of low clay content, by choosing a suitable m from data collections such as Table 1, and, if possible, with the aid of site-specific laboratory calibrations. Two possible generalizations of Archie's Law that involved the addition of an empirical multiplying factor, $\sigma_a/\sigma_w = an^m$ ($a \neq 1$), or the subtraction of a non-contributing fraction of the porosity, $\sigma_a/\sigma_w = (n - n_c)^m$, could have adapted this empirical model to water-saturated soils. However, these modifications were not widely adopted, and will not be discussed here.

One possible constructive physical approach is to resort to the mean field theories mentioned above. The simplest two-phase case is that of finding a homogeneous material with an effective conductivity (σ_a) equal to that of a mixture of conductivity σ_s, composed of similar size solid spheres that occupy a fraction f (=1 − n) of the total volume, immersed randomly in a host conductivity of σ_w and volumetric fraction n. Maxwell (1881) formula is usually written in asymmetric form as:

$$\frac{\sigma_a - \sigma_w}{\sigma_a + 2\sigma_w} = f\frac{\sigma_s - \sigma_w}{\sigma_s + 2\sigma_w} \tag{3}$$

and for the relevant case of non-conducting solid particles ($\sigma_s = 0$), this reduces to

$$\frac{\sigma_a}{\sigma_w} = \frac{2n}{3 - n}. \tag{4}$$

One appealing feature of the Maxwell model is its mathematical simplicity, which perhaps explains why it arises also from other trains of reasoning (Sihvola, 1999). The geometric picture addressed by the Maxwell model, involving similar-sized spheres randomly distributed in a host material, is one of the simplest three-dimensional (3-D) systems conceived. The assumptions underlying the Maxwell mixing formula are apparently also over-simplified. Fig. 2 presents accurate measurements of $\sigma_a/\sigma_w(n)$ in packings of mono-sized glass beads, and the Maxwell model clearly over-predicts the measured conductivities. Nevertheless, surprisingly, this classical model has proven to be a very good predicting tool for many two-phase mixtures (Hanai, 1968; Sihvola, 1999) and even for water-saturated soils (Mualem and Friedman, 1991) and other granular materials (Friedman and Robinson, 2002).

The other mean field theories can be presented (for $\sigma_s = 0$) via a universal mixing law (Sihvola and Kong, 1988):

$$\sigma_a = \sigma_w + \left\{\left[\frac{(n-1)\sigma_w[\sigma_w + a(\sigma_a - \sigma_w)]}{\frac{2}{3}\sigma_w + a(\sigma_a - \sigma_w)}\right]\left[1 - \frac{\frac{1}{3}(n-1)\sigma_w}{\frac{2}{3}\sigma_w + a(\sigma_a - \sigma_w)}\right]^{-1}\right\} \tag{5}$$

which contains a heuristic parameter, a, whose value lies between 0 and 1, which accounts for the effect of neighboring particles on the internal electrical field of a reference particle. The universal model reduces to the Maxwell formula when the value of a is 0 (Eq.

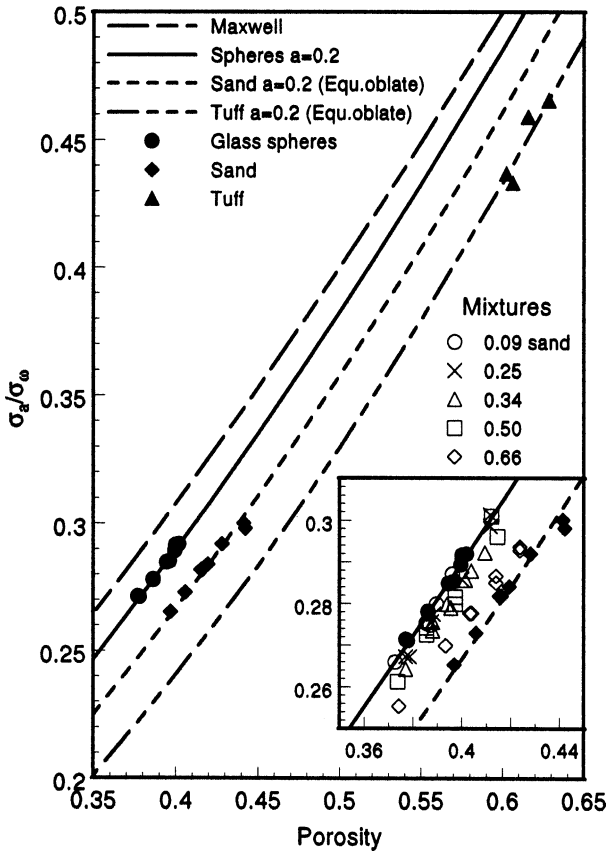

Fig. 2. Reduced apparent electrical conductivity (σ_a/σ_w) as a function of porosity. Lines represent Eq. (9); the value of a fitted to the glass spheres data is 0.2. The main graph shows the glass beads ($a/b = 1$), sand grains ($a/b = 0.460$), and tuff grains ($a/b = 0.350$), where the aspect ratios have been adjusted to fit the data. The inset graph shows data for sand mixed in glass beads (from Friedman and Robinson, 2002; reproduced by permission of the American Geophysical Union, Copyright 2002 AGU).

(5) only apparently diverges for $a = 0$), to the symmetric effective medium approximation (Bruggeman, 1935) for $a = 2/3$, and to the coherent potential formula (Tsang et al., 1985) for $a = 1$. The conductivity $\sigma^* = \sigma_w + a(\sigma_a - \sigma_w)$ can be regarded as that seen outside by the inclusion (solid particle), and it can assume values different from that of the host material, ranging from $\sigma^* = \sigma_w$ for the Maxwell model up to the effective conductivity of the mixture, $\sigma^* = \sigma_a$, for the coherent potential mixing rule. Among the three classical mixing formulas, the Maxwell formula is probably the best predictor of the effective conductivity, at least for granular mixtures saturated with water (and/or other liquids) for which $\sigma_s = 0$ (Friedman and Robinson, 2002; Robinson and Friedman, submitted for publication). Nevertheless, it was recently shown that allowing $a = 0.2$ resulted in better prediction of the σ_a of water-saturated packings of glass beads, sand grains, and tuff particles (Friedman and Robinson, 2002; Fig. 2); it was also more effective for predicting related transport properties

such as the effective dielectric permittivity of glass beads immersed in liquids of different permittivity (Robinson and Friedman, submitted for publication).

Eq. (5) applies to spherical solid particles, but the most important geometrical soil attribute with regard to its $\sigma_a/\sigma_w(n)$ relationship is probably particle shape, which varies from almost spherical sand grains to flat, disk-like and long, needle-like clay tactoids. It is practically impossible to calculate the effective conductivity of packings of angular and rough-surfaced particles, but these features were found to be of secondary importance in their effects on σ_a (Friedman and Robinson, 2002). Representing the particle geometry as an ellipsoid of revolution (spheroid) provides both convenient analytical expressions and sufficient flexibility for transformation into a variety of shapes by altering the aspect ratio (Sihvola and Kong, 1988; Sareni et al., 1997; Jones and Friedman, 2000). By extending or contracting the b and c axes whilst keeping a constant, one can transform a sphere into either a disk-like (oblate) or needle-shaped (prolate) particle, such as are often encountered in the natural environment. Particle shape is then incorporated in σ_a modeling through a parameter named the depolarization factor (N^i), which describes the extent to which the inclusion polarization is reduced according to its shape and orientation with respect to the applied electrical field. For the special cases of ellipsoids of revolution ($a \neq b = c$) Jones and Friedman (2000) found that $N^a(a/b)$ can be satisfactorily approximated ($r^2 = 0.9999$) by a single empirical expression,

$$N^a = \frac{1}{1 + 1.6(a/b) + 0.4(a/b)^2}; \qquad N^b = N^c = \tfrac{1}{2}(1 - N^a) \tag{6}$$

through the whole range of aspect ratios, a/b, from thin disks to long needles. The depolarization factors are: for a sphere, in which a, b, and c are all equal in length, $N^{a,b,c} = 1/3, 1/3, 1/3$; for a thin disk (extreme oblate), 1, 0, 0, respectively; and for a long needle (extreme prolate), 0, 1/2, 1/2, respectively. The particle aspect ratio, a/b, of coarse granular materials can be retrieved from databases, evaluated directly by visual inspection under magnification, or determined indirectly by the simple angle of repose measurement (Friedman and Robinson, 2002).

Non-spherical particles can form either anisotropic or isotropic packings, depending on whether they are aligned in the same direction or are randomly oriented. The effective conductivity of non-spherical particles, aligned to form a uniaxial–anisotropic medium, is no longer a scalar, but is a second-order tensor, defined by its diagonal components $\sigma_a^a \neq \sigma_a^b = \sigma_a^c$. The effective conductivity in the ith direction takes the form (Sihvola and Kong, 1988):

$$\sigma_a^i = \sigma_w + \left\{ \left[\frac{(n-1)[\sigma_w + a(\sigma_a^i - \sigma_w)]\sigma_w}{\sigma_w + a(\sigma_a^i - \sigma_w) - N^i\sigma_w} \right] \cdot \left[1 - \frac{(n-1)N^i\sigma_w}{\sigma_w + a(\sigma_a^i - \sigma_w) - N^i\sigma_w} \right]^{-1} \right\}, \tag{7}$$

(which reduces to Eq. (5) for spheres, $N^i = 1/3$), in which the previously presented mixing parameter, a, accounts for the effect of neighboring particles on the internal electrical field and the newly introduced depolarization factors (N^i) are defined by the particle aspect ratio and their alignment with respect to the applied electrical field. If the effective conductivities in the principal anisotropy directions ($\sigma_a^a, \sigma_a^b, \sigma_a^c$) are known, the effective conductivity

when the electrical field is directed arbitrarily, forming angles β^a, β^b, and β^c relative to the a, b, and c, coordinate axes, respectively, is given by

$$\sigma_{\mathrm{a}}^{\beta} = \sigma_{\mathrm{a}}^{a} \cos^2 \beta^a + \sigma_{\mathrm{a}}^{b} \cos^2 \beta^b + \sigma_{\mathrm{a}}^{c} \cos^2 \beta^c. \tag{8}$$

The above calculations of directional effective conductivity (Eqs. (7) and (8)) apply to perfectly aligned spheroids. The particles in real anisotropic soils are, however, only partially aligned with respect to the principal anisotropy axes. The directional effective conductivities of such media can be calculated by applying similar principles, with the addition of the distribution of the particle (long axis) orientation (Dafalias and Arulanandan, 1979; Arulanandan, 1991; Thevanayagam, 1993).

Even non-spherical particles, when oriented randomly, form an isotropic medium with a scalar effective conductivity, σ_{a}. If we apply a superposition principle, the isotropic version of the universal mixing law, Eq. (5), takes the form (Sihvola and Kong, 1988):

$$\sigma_{\mathrm{a}} = \sigma_{\mathrm{w}} + \left\{ \left[\sum_{i=a,b,c} \frac{(n-1)[\sigma_{\mathrm{w}} + a(\sigma_{\mathrm{a}} - \sigma_{\mathrm{w}})]\sigma_{\mathrm{w}}}{3[\sigma_{\mathrm{w}} + a(\sigma_{\mathrm{a}} - \sigma_{\mathrm{w}}) - N^i \sigma_{\mathrm{w}}]} \right] \times \left[1 - \sum_{i=a,b,c} \frac{(n-1)N^i \sigma_{\mathrm{w}}}{3[\sigma_{\mathrm{w}} + a(\sigma_{\mathrm{a}} - \sigma_{\mathrm{w}}) - N^i \sigma_{\mathrm{w}}]} \right]^{-1} \right\}. \tag{9}$$

Friedman and Robinson (2002) measured the σ_{a} of packings of three kinds of coarse granular materials – glass spheres, sand, and tuff particles – and the data are presented in Fig. 2, which also includes $\sigma_{\mathrm{a}}/\sigma_{\mathrm{w}}(n)$ measurements for glass–sand mixtures. As mentioned above, best-fitting the heuristic mixing parameter (a of Eq. (9)) to the measured $\sigma_{\mathrm{a}}/\sigma_{\mathrm{w}}(n)$ data for the packed spheres again resulted in $a = 0.2$, indicating to some extent its physical significance. In Fig. 2, the aspect ratios of the sand and tuff particles were adjusted to provide a best fit to their $\sigma_{\mathrm{a}}/\sigma_{\mathrm{w}}(n)$ measurements; this gave a/b values of 0.46 and 0.35, respectively, which are remarkably similar to those determined from the slope angle measurements (i.e., 0.48 and 0.33) and to those predicting the effective dielectric permittivity–porosity relationships of these packings (Friedman and Robinson, 2002). This closure is indicative of the merits and physical significance of the empirical relationship between the slope angle and the shape factor, of the choice of an oblate–spheroid geometry to represent the particle shape, and of the heuristic mixing model (Eq. (9)) with $a = 0.2$ for predicting the $\sigma_{\mathrm{a}}/\sigma_{\mathrm{w}}(n)$ relationships of isotropic granular media made of non-spherical particles. Therefore, we recommend using Eq. (9) for predicting the $\sigma_{\mathrm{a}}(\sigma_{\mathrm{w}}, n)$ relationship of coarse-textured soils, provided that a sensible evaluation of the particle aspect ratio (required for calculating the depolarization factors according to Eq. (6)) is possible.

The self-similar model of Sen et al. (1981) for the complex dielectric permittivity of spherical particles can be used for evaluating the "quasi-static" effective EC, which reduces to Bruggeman's (1935) asymmetric effective medium approximation:

$$\left(\frac{\sigma_{\mathrm{s}} - \sigma_{\mathrm{a}}}{\sigma_{\mathrm{s}} - \sigma_{\mathrm{w}}}\right)\left(\frac{\sigma_{\mathrm{w}}}{\sigma_{\mathrm{a}}}\right)^{1/3} = n \tag{10}$$

and for $\sigma_s = 0$ becomes Archie's power law with $m = 3/2$: $\sigma_a/\sigma_w = n^{3/2}$, and therefore, establishes a theoretical basis for the latter. The 3/2 exponent also results from other approaches, e.g., the prediction of the semi-empirical, cut-and-rejoin model of Mualem and Friedman (1991) for coarse media of a narrow pore-size distribution. In cases where nothing is known about the soil, it is recommended to use $\sigma_a/\sigma_w = n^{3/2}$ for evaluating σ_w. The self-similar model (10) can also be extended to non-spherical particles by proper averaging of the depolarization factors (N) over all possible particle orientations; this again results in a form of Archie's power law, with a particle shape-dependent m exponent (Mendelson and Cohen, 1982; their derivation contains an arithmetic mistake, corrected by Sen, 1984):

$$m = \left\langle \frac{5 - 3N}{3(1 - N^2)} \right\rangle. \tag{11}$$

One interesting and significant result of this self-similar mixing modeling is that for isotropic media that comprise prolate particles, the exponent m is restricted to below 5/3 (for randomly oriented long, needle-like particles), whereas for oblate, disk-like particles, m is unbounded. In principle, the self-similar model constitutes a theoretical basis for Archie's power law including non-spherical particles. However, we do not recommend using this approach for evaluating the Archie's law exponent, because the unrealistic self-similar assumption results in insufficient sensitivity to the particle shape: it underestimates $\sigma_a/\sigma_w(n)$ (over-shooting m) for spherical particles and overestimates it for appreciably non-spherical particles. For example, when using the aspect ratios of $a/b = 0.48$ and 0.333 for the sand and tuff particles, respectively (Friedman and Robinson, 2002), the resulting m values for the glass spheres, sand, and tuff particles are 1.5, 1.54, and 1.60, respectively. However, the exponents that best fitted the data (Fig. 2) are 1.35, 1.45, and 1.66, respectively (Table 1).

The reduced effective electrical conductivity, σ_a/σ_w, is dimensionless and cannot, of course, depend on any length scale. Thus, the absolute (mean) soil particle size does not affect the $\sigma_a/\sigma_w(n)$ relationship (when the adsorbed cation contribution to σ_a is disregarded), and it is only the broadness of the particle-size distribution that affects $\sigma_a/\sigma_w(n)$ of coarse-textured soils. Maxwell-Garnett (1904) model formed the basis of the self-similar model derived by Sen et al. (1981), whose main modification involved sequential additions of the inclusion solid phase into the host water phase, while the background pore system remained intact (applicable to most soils). The resulting formula (Eq. (10)) is impressively simple but, nevertheless, this model should apply, in principle, to a fractal medium of infinitely wide particle-size distribution and should, therefore, form a lower limit for the estimated values of σ_a of real water-saturated soils comprising almost spherical grains of bounded particle-size distribution. This has indeed been proven for mixtures of uniform-sized spherical particles. Fig. 3 presents the $\sigma_a/\sigma_w(n)$ measurements for randomly packed uniform spheres and for sequential additions of particles of decreasing diameter (12.7, 9.5, 3.2, and 1.5 mm) randomly packed around a larger 76.2-mm sphere (Robinson and Friedman, submitted for publication). Two additional data sets are presented, determined by Lemaitre et al. (1988), for binary mixtures with size ratios of 4 and 11. All these data show a similar general trend, migrating from Shivola's universal model ($a = 0.2$; Eq. (5)) towards the limit of Sen et al.'s (1981) self-similar model (Eq. (10) simplified to $\sigma_a/\sigma_w = n^{3/2}$) as the broadness of the particle-size distribution increases, accompanied by decreasing porosity.

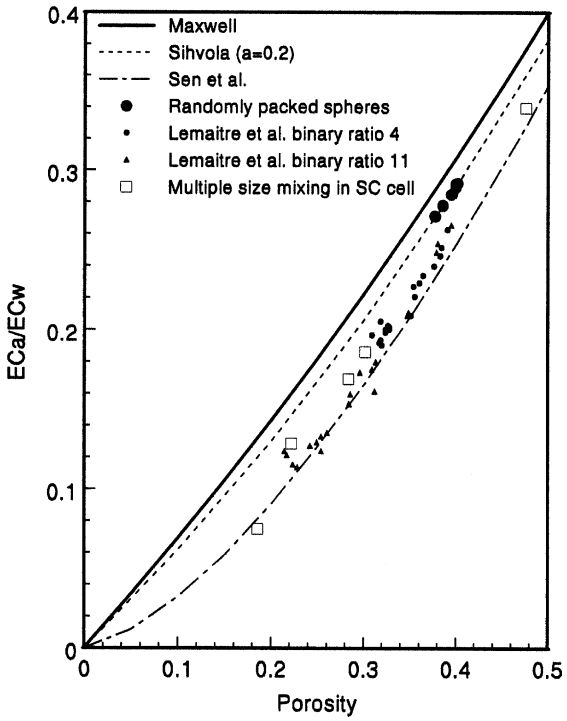

Fig. 3. Reduced apparent electrical conductivity (σ_a/σ_w) of randomly packed mono-sized spheres and of mixtures of spheres of different sizes (from Robinson and Friedman, submitted for publication).

These effects of particle size distribution are less pronounced than those of particle shape and orientation, and for soils suspected to have a broad particle size distribution and consequently relatively low porosities, it is recommended to use Eq. (10) for evaluating σ_w. For perfectly aligned non-spherical particles, the 1/3 exponent in Eq. (10) should be replaced with the depolarization factor (Eq. (6)), which depends on the particle shape and orientation with respect to those of the applied electrical field (Sen et al., 1981). Increasing width of particle size distribution and increasing particle asphericity tend to reduce the porosity of the medium. It should be noted, however, that the effects on σ_a discussed here are beyond this indirect effect, namely how these geometric attributes affect σ_a for a given porosity.

The above discussion, relevant to the evaluation of the soil solution EC from σ_a/σ_w measurements, was based on the assumption of negligible contribution of the adsorbed ions to the overall σ_a—only the structural aspects were considered. For this assumption to be valid, it is necessary either that the soils are coarse-textured (clay free), as discussed above, or that σ_w is sufficiently high to allow σ_a to increase approximately linearly with σ_w and the geometric (intrinsic) formation factor to be determined by extrapolating from several measured $\sigma_a/\sigma_w(\sigma_w)$ values as $\sigma_w \to \infty$ (Waxman and Smits, 1968; Shainberg et

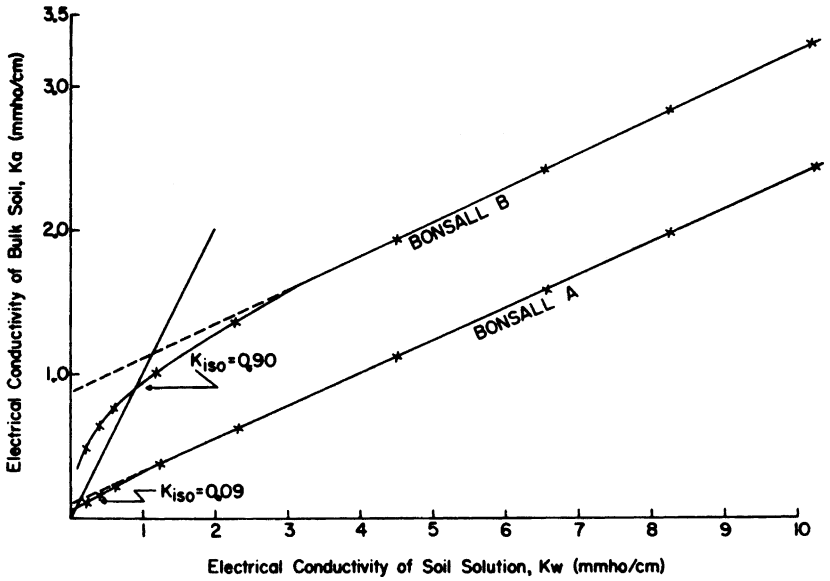

Fig. 4. The apparent electrical conductivity (σ_a) of water-saturated Bonsall soils from the A and B horizons as a function of the electrical conductivity of the soil solution (σ_w). K_{iso} is the isoconductivity point where $\sigma_a = \sigma_w$ (from Shainberg et al., 1980; reproduced by permission of the Soil Science Society of America).

al., 1980; Nadler et al., 1984; Johnson and Sen, 1988; Bernabé and Revil, 1995). In all other extreme and intermediate cases, the $\sigma_a(\sigma_w, n)$ problem is more complex involving additional geometrical (specific surface area/particle size) and chemical (charge density) characteristics of the solid phase, and the ionic strength (σ_w) and composition (prevailing metallic cations and pH) of the rock or soil solution.

Fig. 4 presents the measured $\sigma_a(\sigma_w)$ relationships for two soils with 8% (Bonsall A) and 35.5% (Bonsall B) clay content equilibrated with solutions of SAR = 0 (Shainberg et al., 1980). At relatively saline solutions ($\sigma_w > 4$ dS/m), the two $\sigma_a(\sigma_w)$ functions are linear with similar slopes regardless of the different clay percentage of the two soils (0.225 and 0.235 for the A and B horizons, respectively). At low salinities ($\sigma_w < 4$ dS/m), the $\sigma_a(\sigma_w)$ relationship, especially that of the clayey soil, is highly non-linear. Shainberg et al. (1980) studied the effects of cation exchange capacity and exchangeable sodium percentage (ESP) in conditions of non-linear $\sigma_a(\sigma_w)$ relationships and found that the contribution of the surface conductivity to σ_a, as indicated by the intercept of the tangent line at $\sigma_w = 0$ (Fig. 4), increases with increasing CEC (/clay content). Although less conclusive, the surface conductivity was also found to increase with the ESP (or corresponding SAR) levels. The first direct reason for this is the higher electrical mobility of the adsorbed sodium ions as compared to calcium. A second indirect effect is due to the soil structure: at high ESP (and low σ_w) values, slaking of the soil aggregates occur, and it is not trivial to deduce whether the re-arrangement of the soil particles increases or decreases σ_a. Based on other studies, Rhoades et al. (1999) concluded that the $\sigma_a(\sigma_w)$ relationship does not depend on the soil

ESP (/SAR), provided soil structure and porosity have not been seriously degraded by the sodicity.

In a theoretical study, Schwartz et al. (1989) established σ_a at the two extremes of $\sigma_w = 0$ and $\sigma_w \to \infty$, and the gap was filled by means of a Padé approximant based on four independent measurable geometrical parameters. A comprehensive, rigorous treatment of the $\sigma_a(\sigma_w, n)$ problem under such circumstances would be too extensive for the present review article, and is also not relevant for practical $\sigma_w(\sigma_a, n)$ determinations, because there are too many unknown parameters involved. The interested reader is, therefore, referred to other publications (e.g., Kan and Sen, 1987; Johnson and Sen, 1988; Revil and Glover, 1998; Revil et al., 1998; Schwartz et al., 1989). From the practical point of view, it should be noted that measuring methods such as induced polarization (Lesmes and Frye, 2001) can be applied in the field and have the potential merit of assisting in differentiating the contributions of surface and bulk fluid conductivities to the measured σ_a.

Most soils contain a considerable fraction of (negatively) charged minerals, and σ_w is often sufficiently low for the contribution of the adsorbed counterions (cations) to σ_a to be significant. The most frequently applied simplifying assumption is that σ_a can be regarded as being replaced by two conductors in parallel, one representing the dissolved ions (σ_w/F), and the other the adsorbed ones (σ_s) (Rhoades et al., 1976; Nadler et al., 1984; Mualem and Friedman, 1991):

$$\sigma_a = \frac{\sigma_w}{F} + \sigma_s(\sigma_w). \tag{12}$$

The geometric formation factor (F), which is used to determine σ_w by means of, e.g., Eq. (2), can be deduced by subtracting the estimated surface conductivity (σ_s) from the measured σ_a. In order to avoid confusion, we do not introduce the terminology of an apparent formation factor, defined as overall σ_a over σ_w, which is not a purely geometric factor. The surface conductivity (σ_s) can be regarded as either σ_w-independent, and, therefore, susceptible to estimation by extrapolating the measured $\sigma_a(\sigma_w)$ values to $\sigma_w = 0$ (Rhoades et al., 1976), or as an empirically determined increasing function of σ_w (Waxman and Smits, 1968; Nadler et al., 1984): $\sigma_s(\sigma_w) = \delta\sigma_s^{max}$ ($0 < \delta < 1$). The maximal σ_s value (σ_s^{max}), applicable to high σ_w values within the framework of Eq. (12), can be reliably estimated as the $\sigma_w = 0$ intercept of the straight line, tangential to the linear portion of the plot of measured $\sigma_a(\sigma_w)$ values at high σ_w, if they are available. σ_s^{max} is an increasing function of the clay percentage or CEC, and can be evaluated also from empirical correlations to other easily measured, related textural characteristics, e.g., the hygroscopic water content (Nadler et al., 1984). Several authors have offered simple (Waxman and Smits, 1968) or more sophisticated (Revil and Glover, 1997, 1998; Revil et al., 1998) means for evaluating σ_s^{max} on the basis of surface conduction theories and known chemical characteristics of the mineral surfaces and saturating solution, but these are of limited practical applicability. At $\sigma_w = 0$, σ_s should vanish, in principle ($\delta = 0$). Applying this empirical approach, Waxman and Smits (1968) obtained formation factors that exhibited an Archie's power law dependence, with m exponents of 1.74 for Eocene sand and of 2.43 for lower tertiary sands. Sen et al. (1988) proposed another version of Eq. (12); it refers explicitly to the surface charge density, Q_V (charge per unit pore

volume), and assumes an Archie's law formation factor

$$\sigma_a = n^m \left[\sigma_w + \frac{1.93 m Q_V}{1 + 0.7/\sigma_w} \right], \quad (13)$$

where $1.93m$ (S/m) (L/m) and 0.7 (S/m) are empirical parameters that account for the geometry and reduced cationic mobility near the surfaces with the exponent m as the only free variable. This empirical expression was reasonably successful in describing the $\sigma_a(\sigma_w, n, Q_V)$ relationship of 140 cores of clay-bearing sandstones, with m ranging between 1.8 and 2.3. This is in agreement with the findings of Revil et al. (1998) who found that the corresponding m increased approximately linearly with the CEC, $Q_V n/(1-n)$, from about 1.8 for clean sand and sandstones to about 2.6 for smectite-rich sandstones. Thus, in circumstances where the charge density (clay content) is appreciable and known, it is recommended to use Eq. (13) for porosity and σ_w determination in clay-bearing (shaly) sandstones.

The decoupling assumption embedded in Eqs. (12) and (13) is physically inappropriate for application to a locally heterogeneous medium and its use can lead to a significant over-estimation of σ_w/F, especially for media of high cation-exchange capacity, broad pore-size distribution, and low connectivity (Friedman, 1998). The reason is that the conduction of an electrical current in the bulk soil/rock between the electrodes does not follow two parallel paths, but involves a 3-D network of conductors arranged in a complicated combination of series and parallel connections (Bernabé and Revil, 1995; Friedman, 1998). Only in a single pore can the electrical conduction be regarded as taking place in parallel through the dissolved and adsorbed ions. This limitation applies also to such decoupling models for the $\sigma_a(\sigma_w, \theta)$ relationship of unsaturated soils (e.g., Eqs. (17) and (18)). Several modifications of Eq. (12) have been proposed, to include other conducting elements of solid surfaces and solution in series (Shainberg et al., 1980), and of immobile water (Rhoades et al., 1989), but the approximate representation was still based on macroscopic elements connected in parallel. It should be noted that discrete 3-D (e.g., cylindrical) pore network models are not realistic enough for representing the pore system of granular media of such soils, which is why the expected errors according to Friedman (1998) are probably over-estimated and the parallel assumption works pretty well. Yet, qualitatively, the above statement and the effects of local heterogeneities and surface conductivity are correct.

In the above discussion, it was assumed that the porosity (n) was estimated from, e.g., TDR measurements, and could be used for evaluating σ_w from σ_a readings. In other circumstances, when the σ_w and the relevant material parameters (corresponding to the various models) can be reliably evaluated, the porosity can be determined from σ_a measurements, by means of the same expressions, as listed above. According to Archie's law (Eq. (2)), for example, σ_a is more sensitive to n ($m > 1$) than it is to σ_w. In this respect, $n(\sigma_a, \sigma_w)$ determinations are expected to be more reliable than $\sigma_w(\sigma_a, n)$ determinations. For both σ_w and n determinations, possibly deleterious temperature effects are worth noting: the electrical conductivity of free solution (σ_w) increases by about 2% per 1 °C (around 25 °C, corresponding to the decrease of the free water viscosity) and a similar effect is to be expected for σ_a of coarse-textured media so that the reduced conductivity, σ_a/σ_w, is temperature independent. Thus, it is sufficient to correct both field and/or laboratory σ_a and σ_w measurements to the

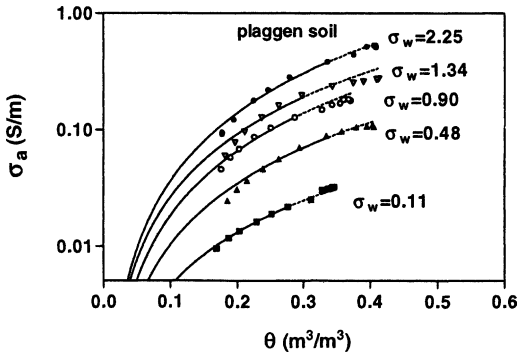

Fig. 5. Measured (symbols) and lines fitted to Eq. (16), $\sigma_a(\sigma_w, \theta)$ data for Plaggen dark loamy sand. The soil solution conductivity, σ_w (S/m), is indicated near each line (from Weerts et al., 1999; reproduced by permission of the American Geophysical Union, Copyright 1999 AGU).

same reference temperature, usually $T = 25\,^{\circ}\mathrm{C}$. A more accurate temperature conversion factor based on a common soil solution composition recommended by the U.S. Salinity Laboratory staff (1954) and Rhoades et al. (1999) is

$$\sigma_w^{25} = f_T \sigma_w^T; \quad f_T = 1 - 0.020346(T - 25) + 0.003822(T - 25)^2 + 0.000555(T - 25)^3. \tag{14}$$

However, in clay-bearing media that exhibit significant surface conduction, the counterion mobility increases more sharply with temperature and the σ_a–temperature relationship is more complex (Clavier et al., 1984; Sen and Goode, 1992; Wraith et al., 1999). Sen and Goode (1992), for example, present slopes from 0.02, corresponding to the slope of free solution, to 0.12 of $\sigma_a(T)$ measurements at high σ_w for shaly sands containing varying amounts of clay. This adds another complication to n or σ_w determinations in such media.

3.2. Unsaturated soils

Time domain reflectometry measurements can be used to determine both the effective permittivity (ε_{eff}) in the GHz range, from which θ can be determined, and the low-frequency σ_a from which σ_w can be evaluated (evaluating θ from measurements of ε_{eff} are more reliable, because the $\varepsilon_{eff}(\theta)$ relationship is more universal, i.e., with smaller variations among different soils types, than the $\sigma_a(\sigma_w)$ relationship). Fig. 5 presents such a set of $\sigma_a(\sigma_w, \theta)$ measurements for a dark (3.5% organic matter) loamy sand (Weerts et al., 1999; note the logarithmic σ_a axis; on linear scales, the $\sigma_a(\theta)$ lines have a positive curvature, e.g., Fig. 8).

The geometrical factors discussed above are relevant also to unsaturated soils; in some cases, these factors are expected to have even more significant effects on $\sigma_a/\sigma_w(\theta)$ than on $\sigma_a/\sigma_w(n)$. One extreme example is shown in Fig. 6 from Friedman and Jones (2001), who measured the directional effective electrical conductivities in directions parallel and perpendicular to the layering plane of anisotropic packings of mica particles with an aspect

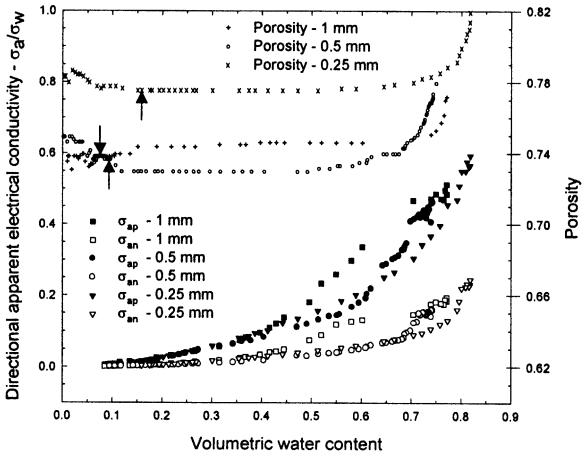

Fig. 6. The directional electrical conductivities and the porosites of three anisotropic mica particle packings of different, denoted size fractions as a function of the volumetric water content. The filled markers are for the parallel (horizontal) σ_a and the empty ones for the normal (vertical) σ_a. The arrows mark the change from suction to evaporative drying (from Friedman and Jones, 2001; reproduced by permission of the American Geophysical Union, Copyright 2001 AGU).

ratio (i.e., diameter/thickness) of about 25. The measurements started with water-saturated packings that were first allowed to reduce their water contents by draining followed by evaporation. The anisotropy factor, defined as the ratio of the conductivities parallel to the bedding plane and perpendicular to it, initially increased moderately as desaturation progressed (geometrical effects increased as saturation decreased), and then decreased as the drier region of residual moisture contents was approached. An anisotropic variant (Friedman and Jones, 2001) of a critical path analysis (Ambegaokar et al., 1971) was used to reconstruct this experimentally determined pattern qualitatively, thus helping to explain the observed dependence of the apparent electrical conductivity's anisotropy factor on the degree of saturation. Extending model equations such as Eqs. (7) and (9) to three phases – solid, water, air – is feasible (Friedman, 1998; Jones and Friedman, 2000), but these three-phase models are still of limited use in prediction, mainly because of the unknown configurations of the liquid and gaseous phases. Therefore, I review mainly empirical and semi-empirical models, commonly used by soil scientists, hydrologists, and geophysicists.

In his seminal article, Archie (1942) already stated that a power law describes the $\sigma_a(S)$ relationship down to water saturations (oil being the non-conducting phase in his case) of about 0.15–0.2: $\sigma_a(S) = \sigma_a(S = 1)S^d$, with an exponent d close to 2 for both consolidated and unconsolidated sands (whether coincidental or not, this exponent is very close to the universal 3-D percolation conductivity exponent: $t = 1.9$ (Katz and Thompson, 1986)). Thus, the extended Archie's law should be written, in general, as:

$$\frac{\sigma_a}{\sigma_w} = n^m S^d. \tag{15}$$

Gorman and Kelly (1990) obtained average best-fitted values of $m = 1.30$ and $d = 1.53$ for various Ottawa sand mixtures. When the degree of saturation decreases, the water films surrounding the solid particles become thinner and the conducting paths become increasingly tortuous. Thus, there is a physical reason for the saturation exponent to be larger than the porosity one: $d > m$. According to the commonly used semi-empirical model of Mualem and Friedman (1991), the geometric formation factor (after subtracting the surface conductivity contribution to σ_a according to Eq. (12)) of coarse-textured media with fairly narrow pore-size distributions results in an expression similar to Eq. (15) with $m = 1 + \lambda$ and $d = 2 + \lambda$. The tortuosity exponent λ can be taken as 0.5, making $m = 1.5$ and $d = 2.5$, or it can be best-fitted to the $\sigma_a/\sigma_w(\theta)$ measurements. The equation can also be written as $\sigma_a/\sigma_w = \theta^{2+\lambda}/n$, and Persson (1997), for example, best-fitted a λ of about 0.2 to $\sigma_a/\sigma_w(\theta)$ measurements in a sand ($n = 0.38$), homogenously packed into short ($\lambda = 0.25$) or long ($\lambda = 0.16$) columns. Mualem and Friedman's model does not refer to the whole liquid phase volume but subtracts from both n and θ a non-contributing volume (θ_0) close to the solid surfaces, which they proposed to estimate as the water content at wilting point (matric pressure of -15 atm) that correlates well with the specific surface area and clay fraction of the soil. An effective degree of saturation is then defined as $S_e \equiv (\theta - \theta_0)/(n - \theta_0)$. Because this model is semi-empirical and involves at least one calibrating parameter, λ (potentially also θ_0, and some researchers refer to n as an additional free parameter), it is not superior to other, simpler empirical functions. Amente et al. (2000), for example, obtained a better fit to measurements in a sandy loam with a power function of θ alone disregarding n ($\sigma_a/\sigma_w = \theta^{1.58}$). For the general case, the formation factor depends on the pore-size distribution of the medium, as inferred from its water retention characteristics, $\Psi(\theta)$ ($\Psi(m)$ being the matric head), and a tortuosity factor, θ^{λ},

$$\frac{\sigma_a}{\sigma_w} = \theta^{\lambda} \frac{\left[\int_0^{S_e} dS_e/\Psi\right]^2}{\int_0^{S_e} dS_e/\Psi^2} \tag{16}$$

in which the tortuosity exponent is taken as 0.5 (Mualem and Friedman, 1991) or is best-fitted to the $\sigma_a/\sigma_w(\theta)$ and $\Psi(\theta)$ measurements (Weerts et al., 1999). The $\sigma_a(\sigma_w, \theta)$ data of Fig. 5 together with a measured water retention curve, $\Psi(\theta)$, were fit to Eq. (16) and yielded a tortuosity exponent $\lambda = -0.224$.

An earlier attempt to relate the $\sigma_a/\sigma_w(\theta)$ relationship to the pore-size distribution was made by Nadler (1982) who noticed that the formation factor–water content function, $F(\theta)$, resembles the shape of the soil water retention curve, $\Psi(\theta)$ (Fig. 7). Therefore, he suggested the use of an expression of the form $F(\theta) = a\Psi$ (in which a is an empirically determined proportionality constant) for the relatively dry region, while for the relatively wet region, he suggested using Burger's (1919) two-phase mixing law, arbitrarily extended to an unsaturated soil: $F(\theta) = 1 + k(1 - \theta)/\theta$ in which k is an empirically determined, S-independent particle shape factor. Fig. 7 presents an example of such measured and calculated formation factors for a sandy loam (17% clay, 40% silt), packed to a bulk density of 1.45 g cm^{-3}, for which a value of $k = 2.38$ was best-fit to the formation factors over a range of water contents near saturation.

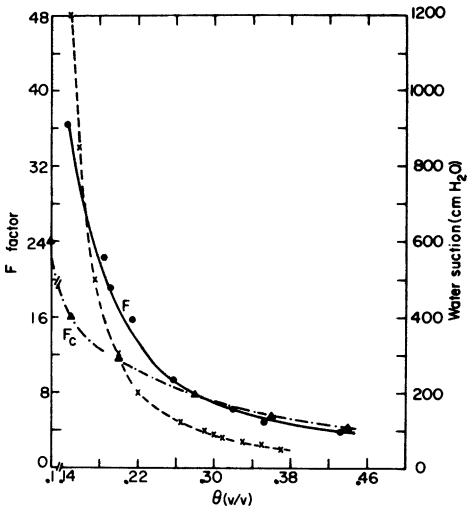

Fig. 7. The measured formation factor for Gilat sandy loam (F, solid circles, solid line), the formation factor calculated according to Burger's (1919) model: $F_c = 1 + 2.38(1-\theta)/\theta$ (solid triangles, dash-dotted line), and the suction (matric) head ("x" markers, dashed line) as a function of volumetric water content (θ) (from Nadler, 1982; reproduced by permission of the Soil Science Society of America).

Among empirical functions proposed by soil scientists for describing the $\sigma_a(\sigma_w, \theta)$ relationship, the most commonly used is that of Rhoades et al. (1976) who referred to σ_s as essentially independent of θ and σ_w and wrote Eq. (12) as:

$$\sigma_a = T(\theta)\theta\sigma_w + \sigma_s, \quad \text{where} \quad T(\theta) = a\theta + b. \tag{17}$$

The transmission coefficient (T) is assumed to be a linear function of θ. The empirical parameters a and b varied among different soils: $a = 2.1$, $b = -0.25$ for clay soils; and $a = 1.3$–1.4, $b = -0.11$ to -0.06 for the other three loam soils discussed in their 1976 article. An example of a transmission coefficient, best-fitted to $\sigma_a(\sigma_w, \theta)$ measurements in a very fine sandy loam (6% clay, 52% silt) is presented in Fig. 8 with $T(\theta)\theta = 1.2867\theta^2 - 0.1158\theta$ plotted. It is seen that $T(\theta)\theta$ is indeed a parabolic function of θ, virtually independent of σ_w. The simplified, two-conductor model (Eq. (17)) should be valid for only saline conditions of approximately $\sigma_w > 4$ dS/m, where the $\sigma_a(\sigma_w)$ relationship is practically linear (e.g., Fig. 4).

Subsequently, Rhoades et al. (1989) extended this empirical model to account for mobile, continuous and immobile, discontinuous aqueous phases, and also allowed for different parallel and series solid–liquid conducting pathways. In these respects, this model somewhat resembles the dual-water model of Clavier et al. (1984) and the parallel–series models of Sauer et al. (1955), Waxman and Smits (1968), and Shainberg et al. (1980) for water-saturated media. Rhoades et al. (1989) referred to three conducting paths acting in parallel: (1) alternating layers of series-coupled solid–liquid (the aqueous phase in the fine pores), (2) solid element (conductance along the surfaces of the soil particles), and (3) continuous liquid element (the aqueous phase in the larger pores). They claimed that the contribution of the solid element is negligible because soil structure does not allow for enough direct

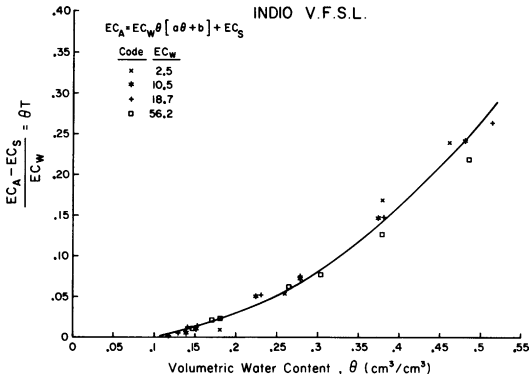

Fig. 8. Plot of $(\sigma_a - \sigma_s)/\sigma_w$ (=$T(\theta)\theta$) according to Eq. (17) of measured $\sigma_a(\sigma_w, \theta)$ data for Indio, very fine sandy loam equilibrated with solutions of different σ_w (given in dS/m). The solid line represents Eq. (17) with the best-fitted transmission coefficient: $T(\theta) = 1.2867\theta - 0.1158$ (from Rhoades et al., 1976; reproduced by permission of the Soil Science Society of America).

particle-to-particle contact and proposed the simplified, two-pathway model:

$$\sigma_a = \frac{(\theta_s + \theta_{ws})^2 \sigma_{ws}\sigma_s}{\theta_s\sigma_{ws} + \theta_{ws}\sigma_s} + (\theta - \theta_{ws})\sigma_{wc} \tag{18}$$

where θ_s is the volumetric fraction of the solid phase (=$1 - n$), θ_{ws} the volumetric water content of the series-coupled solid–liquid element, $(\theta - \theta_{ws})$ the volumetric fraction of the continuous liquid phase, σ_{ws} the conductivity of the soil water of the series-coupled solid–liquid element, σ_s is the conductivity of the solid phase of the solid–liquid element and σ_{wc} of the continuous liquid phase. The greater flexibility of the 1989 model allows for a better description of $\sigma_a(\sigma_w, \theta)$ measurements, especially at low salinities (σ_w), and water contents (θ). However, the increased number of difficult-to-obtain, empirical parameters limits its capacity for predicting $\sigma_w(\sigma_a, \theta)$. Rhoades et al. (1989) presented empirical relationships of two important parameters of their model (θ_{ws} and σ_s) to the respective properties of total volumetric water content (θ) and clay percent (%C): $\theta_{ws} = 0.468\theta + 0.064$ and σ_s (dS/m) = $0.023\%C - 0.0209$. Fig. 9 presents a best-fit of Eq. (18) to a combined $\sigma_a(\sigma_w,\theta)$ data set for a loamy soil (20% clay, 39% silt), assuming $\sigma_{ws} = \sigma_{wc}$ (=σ_w), but it is unclear to what extent these relationships are general or soil specific. Even for detailed models such as Eq. (18), the $\sigma_w(\sigma_a, \theta)$ assessment is expected to be more accurate for high θ. Therefore, Rhoades et al. (1989) recommended $\sigma_a(\theta)$ measurements at higher water contents (i.e., field capacity), when possible, for assessing the amount of dissolved salts in the soil solution (σ_w).

Nadler (1991) studied the effect of soil structure on σ_a by comparing $\sigma_a(\theta)$ data of "field", "packed", and "severely disturbed" samples of four soil types at low and high salinities. The three kinds of samples had similar water contents and they differed moderately and non-systematically in their σ_a, which led him to conclude that severely disturbing processes of sampling, grinding, sieving, and packing have limited effect on the soil's $\sigma_a(\sigma_w, \theta)$ relationship, as long as the soil is re-packed to its original field bulk density. Recognizing

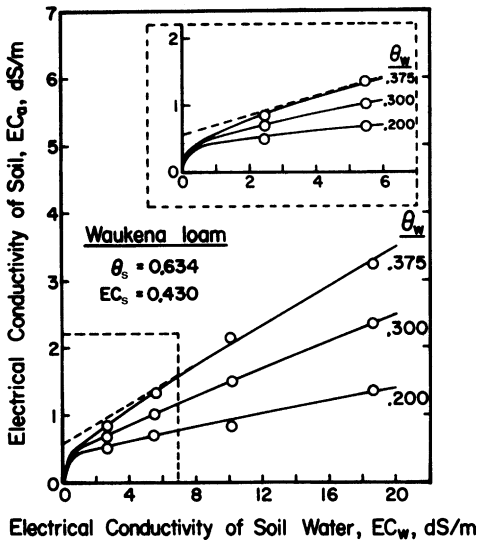

Fig. 9. The apparent electrical conductivity (σ_a) of Waukena loam as a function of solution's electrical conductivity (σ_w) for three volumetric water contents (θ). The empty circles are the measured data, and the solid lines are best-fitted model (with $\theta_s = 0.634$, $\sigma_s = 0.430$ dS/m; Eq. (18)) to the combined data (from Rhoades et al., 1989. Reproduced by permission of the Soil Science Society of America).

that the soil structure defines the orientation and inter-spacing of the soil's primary particles suggests that it should also affect significantly its $\sigma_a(\sigma_w, \theta)$ relationship. Therefore, care should be taken when inferring from $\sigma_a(\sigma_w, \theta)$ calibration curves measured on disturbed, re-packed samples in the lab to the expected $\sigma_a(\sigma_w, \theta)$ relationships of the undisturbed field soil.

Detailed network models are not useful as predictive tools because too many parameters are involved. However, they can provide insight into the nature of the $\sigma_a/\sigma_w(n, \theta)$ problem and can demonstrate the role of structural and other factors in determining σ_a/σ_w. Tsakiroglou and Fleury (1999), who used a bond percolation process for describing drainage in a 3-D cubic network of lamellar pores with fractal roughness, demonstrated that the saturation exponent (d in Eq. (15)) is not S-independent as inferred from Archie's empirical law, but rather increases with decreasing saturation degree from about 1.4 at full saturation to about 3.4 at $S = 0.02$. The main concern of the study of Tsakiroglou and Fleury (1999) was the effect of fractional wettability, when some of the pores are water-wet (the default case discussed above and throughout this chapter) and others are oil-wet. By means of their fractionally wet pore networks, they demonstrated that $\sigma_a(S)/\sigma_a(S = 1)$ is, as expected, always an increasing function of S, and that the saturation exponent (d) is no longer a monotonically decreasing function of S (as for the water-wet media), but exhibits a peculiar behavior that involves an initial decrease of d with decreasing S near saturation, followed by a rise to a local maximum at intermediate degrees of saturation and finally monotonic increasing towards low water saturations. In another network modeling study, Man and Jing (2001) incorporated pore-scale displacement mechanisms (snap-off versus piston-like displacement)

and the full range of advancing contact angles (0–180°) in grain-boundary pore shapes to investigate the behavior of the formation factor in the processes of primary drainage, imbibition, and secondary drainage. The simulated $F(S)$ curves were not linear on a log–log plot (disobeying Archie's law) and showed pronounced hysteresis: σ_a in primary drainage was always larger than that in the following imbibition and secondary drainage cycles, with the differences increasing with increasing contact angles after the primary water drainage. Bekri et al. (2003) calculated the $\sigma_a(S)$ curves of reconstructed 3-D porous media for which the simultaneous flow of two – conducting and insulating – phases (of viscosity ratios of 1.25 and 10) were modeled by means of a Lattice–Boltzmann algorithm. The saturation exponent (d) was in the range of 3–5 and, in general, was virtually S-independent, increasing with decreasing n among the six samples (n of 0.26–0.44) and varying in a complex manner in different spatial directions (parallel and perpendicular to the liquid flows) and for different viscosity ratios. The effects of wettability (contact angle hysteresis), viscosity ratio, flow direction, and imbibition-drainage history have significant implications for the calculation of water/oil saturations from σ_a measurements in oil reservoirs. Agricultural soils of medium to low organic matter content are usually hydrophilic, and wettability effects on σ_a are expected to be negligible. However, in soils containing larger amounts of organic matter, or in other circumstances when even sandy soils can become water repellent (Ritsema et al., 1993), wettability and water flow history issues are expected to affect the $\sigma_a/\sigma_w(\theta)$ relationship.

Most of the soil scientists cited above, and others too, have proposed, tested, and used $\sigma_a(\sigma_w, n, \theta)$ relationships for the purpose of σ_w determination. However, because exponents for the extended Archie's law (15) (m and d) are larger than unity, the σ_a reading is more sensitive to n and $S(\theta)$ than it is to σ_w. Hence, assuming that σ_w and n are known, it is legitimate to estimate θ too from σ_a readings.

4. Conclusion

Experimental evidence and theoretical results have been presented and discussed with the aim of improving our understanding of the roles of the various geometrical and interfacial attributes of the soil and its solution, in determining the effective electrical conductivity of the soil (EC_a). The soil solution EC and the soil volumetric water content are the main factors affecting the soil EC_a, the dependence on water content being stronger. Non-spherical particle shapes and broad particle-size distributions tend to decrease EC_a, and when the non-spherical particles have some preferential alignment in space, the soil is anisotropic, that is, the EC_a depends on the direction in which it is measured. The electrical conductivity of the adsorbed counterions constitutes a major contribution to the EC_a of medium- and fine-textured soils, especially in conditions of low solution conductivity. In such soils and salinity levels, the temperature response of the soil EC_a is likely to be stronger than that of its free solution, and care should be taken when transforming the field-measured EC_a values to the EC_a at a reference temperature.

These findings set some limitations to the application of existing EC_a–EC_w models and constitute guidelines for the further development of such essential models. The best modeling approach is probably that of continuous mean field theories accounting for the major

geometrical and phase configuration attributes when describing the contribution of the dissolved ions and accounting for the mineral surface properties and solution chemistry when describing the contribution of the adsorbed counterions. As such detailed physical models involves numerous soil and environmental attributes, which are usually not readily available to the practitioners, it is essential to seek for general or site-specific inter-correlations between these attributes. Before such reliable physical models are being developed and verified and when accurate EC_w determinations are required, it is recommended to perform site-specific $EC_a(EC_w, \theta)$ calibrations in the laboratory.

References

Adler, P.M., Jacquin, C.G., Thovert, J.F., 1992. The formation factor of reconstructed porous media. Water Resour. Res. 28, 1571–1576.

Ambegaokar, V., Halperin, N.I., Langer, J.S., 1971. Hopping conductivity in disordered systems. Phys. Rev. B 4, 2612–2620.

Amente, G., Baker, J.M., Reece, C.F., 2000. Estimation of soil solution electrical conductivity from bulk soil electrical conductivity in sandy soils. Soil Sci. Soc. Am. J. 64, 1931–1939.

Archie, G.E., 1942. The electrical resistivity log as an aid in determining some reservoir characteristics. Trans. Am. Inst. Min. Metall. Pet. Eng. 146, 54–62.

Arulanandan, K., 1991. Dielectric method for prediction of porosity of saturated soil. J. Geotech. Eng. 117, 319–330.

Balberg, I., 1986. Excluded-volume explanation of Archie's law. Phys. Rev. B 33, 3618–3620.

Bekri, S., Howard, J., Muller, J., Adler, P.M., 2003. Electrical resistivity index in multiphase flow through porous media. Transport Porous Media 51, 41–65.

Bernabé, Y., Revil, A., 1995. Pore-scale heterogeneity, energy dissipation and the transport properties of rocks. Geophys. Res. Lett. 22, 1529–1532.

Briggs, L.J., 1899. Electrical instruments for determining the moisture, temperature, and soluble salts content of soils. USDA Div. Soils Bull. 10, U.S. Gov. Print. Office, Washington, DC.

Bruggeman, D.A.G., 1935. The calculation of various physical constants of heterogeneous substances: I. The dielectric constants and conductivities of mixtures composed of isotropic substances. Ann. Phys. 24, 636–664 (in German).

Burger, H.C., 1919. Das leitvermögen verdünnter mischkristallfreien Legierungen. Physikalische Zeitschrift 20, 73–75 (in German).

Clavier, C., Coates, G., Dumanoir, J., 1984. Theoretical and experimental bases for the dual-water model for interpretation of shaly sands. Soc. Pet. Eng. J. 24, 153–168.

Corwin, D.L., Lesch, S.M., 2005. Apparent soil electrical conductivity measurements in agriculture. Comput. Electron. Agric. 46, 11–43.

Dafalias, Y.F., Arulanandan, K., 1979. Electrical characterization of transversly isotropic sands. Arch. Mech. 31, 723–739.

Dalton, F.N., Herkelrath, W.N., Rawlins, D.S., Rhoades, J.D., 1984. Time domain reflectometry: simultaneous measurement of soil water content and electrical conductivity with a single probe. Science 224, 989–990.

de Kuijper, A., Sandor, R.K.J., Hofman, J.P., de Waal, J.A., 1996. Conductivity of two-component systems. Geophysics 61, 162–168.

Doyen, P.M., 1988. Permeability, conductivity, and pore geometry of sandstones. J. Geophys. Res. 93 (B7), 7729–7740.

Fatt, I., 1956. The network model of porous media: III. Dynamic properties of networks with tube radius distribution. Pet. Trans. AIME 207, 164–177.

Friedman, S.P., 1998. Simulation of a potential error in determining soil salinity from measured apparent electrical conductivity. Soil Sci. Soc. Am. J. 62, 593–599.

Friedman, S.P., Jones, S.B., 2001. Measurement and approximate critical path analysis of the pore scale-induced anisotropy factor of an unsaturated porous medium. Water Resour. Res. 37, 2929–2942.

Friedman, S.P., Robinson, D.A., 2002. Particle shape characterization using angle of repose measurements for predicting the effective permittivity and electrical conductivity of saturated granular media. Water Resour. Res. 38, doi:10.1029/2001WR000746.

Friedman, S.P., Seaton, N.A., 1996. On the transport properties of anisotropic networks of capillaries. Water Resour. Res. 32, 339–347.

Friedman, S.P., Seaton, N.A., 1998. Critical path analysis of the relationship between permeability and electrical conductivity of 3-dimensional pore networks. Water Resour. Res. 34, 1703–1710.

Friedman, S.P., Zhang, L., Seaton, N.A., 1995. Gas and solute diffusion coefficients in pore networks and its description by a simple capillary model. Transport Porous Media 19, 281–301.

Gorman, T., Kelly, W.E., 1990. Electrical–hydraulic properties of unsaturated Ottawa sands. J. Hydrol. 118, 1–18.

Hanai, T., 1968. Electrical properties of emulsions. In: Sherman, P. (Ed.), Emulsion Science. Academic Press, London, pp. 353–478 (Chapter 5).

Hendrickx, J.M.H., Das, B., Corwin, D.L., Wraith, J.M., Kachanoski, R.G., 2002. Relationship between soil water solute concentration and apparent soil electrical conductivity. In: Dane, J.H., Topp, G.C. (Eds.), Methods of Soil Analysis: Part 4. Physical Methods. Soil Science Society of America, Madison, WI, USA, pp. 1275–1282.

Jackson, P.D., Smith, D.T., Stanford, P.N., 1978. Resistivity–porosity–particle shape relationships for marine sands. Geophysics 43, 1250–1268.

Johnson, D.L., Sen, P.N., 1988. Dependence of the conductivity of a porous medium on electrolyte conductivity. Phys. Rev. B 37, 3502–3510.

Jonas, M., Schopper, J.R., Schön, J.H., 2000. Mathematical–physical reappraisal of Archie's first equation on the basis of a statistical network model. Transport Porous Media 40, 243–280.

Jones, S.B., Friedman, S.P., 2000. Particle shape effects on the effective permittivity of anisotropic or isotropic media consisting of aligned or randomly oriented ellipsoidal particles. Water Resour. Res. 36, 2821–2833.

Kadanoff, L.P., 1966. Scaling laws for Ising models near T_c. Physics 2, 263–272.

Kan, R., Sen, P.N., 1987. Electrolyte conduction in periodic arrays of insulators with charges. J. Chem. Phys. 86, 5748–5756.

Katz, A.J., Thompson, A.H., 1986. Quantitative prediction of permeability in porous rock. Phys. Rev. B 34, 8179–8181.

Kirkpatrick, S., 1973. Percolation and conduction. Rev. Mod. Phys. 45, 574–588.

Lemaitre, J., Troadec, J.P., Bideau, D., Gervois, A., Bougault, E., 1988. The formation factor of the pore space of binary mixtures of spheres. J. Appl. Phys. 21, 1589–1592.

Lesch, S.M., 2005. Sensor-directed spatial response sampling designs for characterizing spatial variation of soil properties. Comp. Electron. Agric. 46, 153–179.

Lesmes, D.P., Frye, K.M., 2001. Influence of pore fluid chemistry on the complex conductivity and induced polarization responses of Berea sandstone. J. Geophys. Res. B 106, 4079–4090.

Man, H.N., Jing, X.D., 2001. Network modeling of strong and intermediate wettability on electrical resistivity and capillary pressure. Adv. Water Resour. 24, 345–363.

Maxwell, J.C., 1981. A Treatise on Electricity and Magnetism, vol. 2, second ed. Clarendon Press, Oxford.

Maxwell-Garnett, J.C., 1904. Colours in metal glasses and in metal films. Trans. R. Soc. Lond. 203, 385–420.

Mendelson, K.S., Cohen, M.H., 1982. The effect of grain anisotropoy on the electrical properties of sedimentary rocks. Geophysics 47, 257–263.

Mualem, Y., Friedman, S.P., 1991. Theoretical prediction of electrical conductivity in saturated and unsaturated soil. Water Resour. Res. 27, 2771–2777.

Nadler, A., 1982. Estimating the soil water dependence of the electrical conductivity soil solution/electrical conductivity bulk soil ratio. Soil Sci. Soc. Am. J. 46, 722–726.

Nadler, A., 1991. Effect of soil structure on bulk soil electrical conductivity (EC_a) using the TDR and 4P techniques. Soil Sci. 152, 199–203.

Nadler, A., Frenkel, H., Mantell, A., 1984. Applicability of the four-probe technique under extremely variable water contents and salinity distributions. Soil Sci. Soc. Am. J. 48, 1258–1261.

Pengra, D.B., Wong, P.Z., 1999. Low-frequency AC electrokinetics. Colloids Surf. A: Physicochem. Eng. Aspects 159, 283–292.

Persson, M., 1997. Soil solution electrical conductivity measurements under transient conditions using time domain reflectometry. Soil Sci. Soc. Am. J. 61, 997–1003.

Revil, A., Cathles III, L.M., 1999. Permeability of shaly sands. Water Resour. Res. 35, 651–662.

Revil, A., Cathles III, L.M., Losh, S., Nunn, J.A., 1998. Electrical conductivity in shaly sands with geophysical applications. J. Geophys. Res. 103 (B10), 23925–23936.

Revil, A., Glover, P.W.J., 1997. Theory of ionic-surface electrical conduction in porous media. Phys. Rev. B 55, 1757–1773.

Revil, A., Glover, P.W.J., 1998. Nature and surface electrical conductivity in natural sands, sandstones, and clays. Geophys. Res. Lett. 25, 691–694.

Revil, A., Hermitte, D., Spangenberg, E., Cocheme, J.J., 2002. Electrical properties of zeolitized volcaniclastic materials. J. Geophys. Res. B, doi:10.1029/2001JB000599.

Rhoades, J.D., Chanduvi, F., Lesch, S., 1999. Soil salinity assessment: methods and interpretation of electrical conductivity measurements. FAO Irrigation and Drainage Paper No. 57. Food and Agriculture Organization of the United Nations, Rome, Italy.

Rhoades, J.D., Ingvalson, R.D., 1971. Determining salinity in field soils with soil resistance measurements. Soil Sci. Soc. Am. Proc. 35, 54–60.

Rhoades, J.D., Manteghi, N.A., Shouse, P.J., Alves, W.J., 1989. Soil electrical conductivity and soil salinity: new formulations and calibrations. Soil Sci. Soc. Am. J. 53, 433–439.

Rhoades, J.D., Ratts, P.A.C., Prather, R.J., 1976. Effects of liquid-phase electrical conductivity, water content, and surface conductivity on bulk soil electrical conductivity. Soil Sci. Soc. Am. J. 40, 651–655.

Rhoades, J.D., van Schilfgaarde, J., 1976. An electrical conductivity probe for determining soil salinity. Soil Sci. Soc. Am. J. 40, 647–650.

Ritsema, C.J., Dekker, L.W., Hendrikx, J.M.H., Hamminga, W., 1993. Preferential flow mechanism in a water repellent sandy soil. Water Resour. Res. 29, 2183–2193.

Robinson, D.A., Friedman, S.P. Electrical conductivity and dielectric permittivity of sphere packing: measurements and modelling of cubic lattices, randomly packed monosize spheres and multi-size mixtures. Physica A, submitted for publication.

Robinson, D.A., Jones, S.B., Wraith, J.M., Or, D., Friedman, S.P., 2003. A review of advances in dielectric and electrical conductivity measurement using time domain reflectometry: simultaneous measurement of water content and bulk electrical conductivity in soils and porous media. Vadose Zone J. 2, 444–475.

Sahimi, M., 1994. Applications of Percolation Theory. Taylor and Francis, Bristol, UK.

Sahimi, M., Hughes, B.D., Scriven, L.E., Davis, H.T., 1983. Real-space renormalization and effective-medium approximation to the percolation conduction problem. Phys. Rev. B 28, 307–311.

Sareni, B., Krähenbühl, L., Beroual, A., Brosseau, C., 1997. Effective dielectric constant of random composite materials. J. Appl. Phys. 81, 2375–2383.

Sauer Jr., M.C., Southwick, P.E., Spiegler, K.S., Wyllie, M.R.J., 1955. Electrical conductance of porous plugs: ion exchange resin-solution systems. Ind. Eng. Chem. 47, 2187–2193.

Schwartz, L.M., Kimminau, S., 1987. Analysis of electrical conduction in the grain consolidated model. Geophysics 52, 1402–1411.

Schwartz, L.M., Sen, P.N., Johnson, D.L., 1989. Influence of rough surfaces on electrolyte conduction in porous media. Phys. Rev. B 40, 2450–2458.

Sen, P.N., Scala, C., Cohen, M.H., 1981. A self-similar model for sedimentary rocks with application to the dielectric constant of fused glass beads. Geophysics 46, 781–795.

Sen, P.N., 1984. Grain shape effects on dielectric and electrical properties of rocks. Geophysics 49, 586–587.

Sen, P.N., Goode, P.A., Sibbit, A., 1988. Electrical conduction in clay bearing sandstones at low and high salinities. J. Appl. Phys. 63, 4832–4840.

Sen, P.N., Goode, P.A., 1992. Influence of temperature on electrical conductivity of shaly sands. Geophysics 57, 89–96.

Shainberg, I., Rhoades, J.D., Prather, R.J., 1980. Effect of ESP, cation exchange capacity, and soil solution concentration on soil electrical conductivity. Soil Sci. Soc. Am. J. 44, 469–473.

Sihvola, A., 1999. Electromagnetic Mixing Formulas and Applications. IEE Electromagnetic Waves Series No. 47. Institution of Electrical Engineers, Stevenage, Herts, UK.

Sihvola, A., Kong, J.A., 1988. Effective permittivity of dielectric mixtures. IEEE Trans. Geosci. Remote Sens. 26, 420–429.

Smith-Rose, R.L., 1933. The electrical properties of soil for alternating currents at radio frequencies. Proc. R. Soc. Lond. 140, 359–377.

Stauffer, D., Aharony, A., 1992. Introduction to Percolation Theory. Taylor and Francis, London, UK.

Thevanayagam, S., 1993. Electrical response of two-phase soil: theory and applications. J. Geotech. Eng. 119, 1250–1275.

Topp, G.C., Davis, J.L., Annan, A.P., 1980. Electromagnetic determination of soil water content: measurements in coaxial transmission lines. Water Resour. Res. 16, 574–582.

Torquato, S., 2002. Random Heterogeneous Materials: Microstructure and Macroscopic Properties. Springer-Verlag, New York.

Tsakiroglou, C.D., Fleury, M., 1999. Resistivity index of fractional wettability porous media. Pet. Sci. Eng. 22, 253–274.

Tsang, L., Kong, J.A., Shin, R.T., 1985. Theory of Microwave Remote Sensing. John Wiley, New York.

U.S. Salinity Laboratory Staff, 1954. Diagnosis and improvement of saline and alkali soils. In: Richards, L.A. (Ed.), USDA Agriculture Handbook, vol. 60. U.S. Print Office, Washington, DC, available online at www.ussl.ars.usda.gov.

Waxman, M.H., Smits, L.J.M., 1968. Electrical conductivities and oil-bearing shaly sands. Soc. Pet. Eng. J. 8, 107–122.

Weerts, A.H., Bouten, W., Verstraten, J.M., 1999. Simultaneous measurement of water retention and electrical conductivity in soils: testing the Mualem–Friedman tortuosity model. Water Resour. Res. 35, 1781–1787.

Wenner, F., 1915. A method of measuring Earth resistivity. U.S. Dept. Com. Bureau of Standards Sci. Paper No. 258. NIST, Gaithersburg, MD.

Wraith, J.M., Or, D., 1999. Temperature effects on soil bulk dielectric permittivity measured by time domain reflectometry: experimental evidence and hypothesis. Water Resour. Res. 35, 361–369.

Wraith, J.M., Robinson, D.A., Jones, S.B., Long, D.S., 2005. Spatially characterizing apparent electrical conductivity and water contents of surface soils with time domain reflectometry. Comp. Electron. Agric. 46, 239–261.

Wyllie, M.R.J., Gregory, A.R., 1955. Fluid flow through unconsolidated porous aggregates: effect of porosity and particle shape on Kozeny–Carman constants. Ind. Eng. Chem. 47, 1379–1388.